

This is the peer reviewed version of the following article:

Construction and evaluation of a disposable pH sensor based on a large core plastic optical fiber / Rovati, Luigi; Fabbri, Paola; Luca, Ferrari; Francesco, Pilati. - In: REVIEW OF SCIENTIFIC INSTRUMENTS. - ISSN 0034-6748. - ELETTRONICO. - 82:2(2011), pp. 023106-023106. [10.1063/1.3541795]

Terms of use:

The terms and conditions for the reuse of this version of the manuscript are specified in the publishing policy. For all terms of use and more information see the publisher's website.

18/12/2025 03:51

Construction and evaluation of a disposable pH sensor based on a large core plastic optical fiber

Luigi Rovati,¹ Paola Fabbri,² Luca Ferrari,¹ and Francesco Pilati²

¹*Department of Information Engineering, University of Modena and Reggio Emilia, Modena 41100, Italy*

²*Department of Materials and Environmental Engineering, University of Modena and Reggio Emilia, Modena 41100, Italy*

(Received 5 August 2010; accepted 21 December 2010; published online 16 February 2011)

The fabrication and characterization of a disposable optical fiber sensor for the detection of pH in the range 5–8 are described. The sensing element is a drop of sol–gel hybrid material containing phenol red and deposited onto the tip of a large core plastic optical fiber. This fiber is also exploited for the optical interrogation. This probe can be used as a disposable part of a measuring system. The dynamic range and temporal response of the sensor are here investigated. © 2011 American Institute of Physics. [doi:10.1063/1.3541795]

I. INTRODUCTION

The monitoring of pH (Latin: pondus hydrogenii) level is of great interest in medicine,¹ food industry,² chemical industry,³ marine research,⁴ and wastewater treatment.⁵ Especially in medical applications, the probe disposability is an appreciated quality.⁶ Different types of pH sensors, such as indicator strips, pH electrodes, and optical sensors, are commercially available, but only few of these sensing approaches are suitable for the fabrication of disposable sensing elements.

The design of disposable sensors involves a key aspect related to the implementation of a cheaper and simple transduction mechanism, which converts the information of interest into a readable signal. The advent of large core and low-cost (less than 0.5 \$/m) plastic optical fibers (POFs) on the market makes the interrogation of a colorimetric sensing matrix simple and economic.

The realization of pH sensors through the immobilization of a pH sensitive dye onto the tip or onto the sides of traditional silica-cored optical fibers by means of the sol–gel technology is an already well-known approach.⁷ The sol–gel technique, which consists of a process involving a solution (sol) undergoing a sol–gel solidification, is appropriate in order to realize the sensing matrix to be coupled to POFs. It is actually very simple, not expensive and the resulting matrix is inert, intrinsically bondable to a POF and resistant to aggressive environments.

The traditional fully inorganic sol–gel process offers a mild route for the preparation of porous glass substrates, where pH sensitive dyes can be easily entrapped in. This procedure allows the creation of Si–O–Si linkages between the silica core of the optical fiber and the silica porous matrix deriving from the jellification of the sensitive dye-doped colloidal suspension.⁸ However, this approach cannot be easily applied in the case of plastic optical fibers, due to the ineffective interaction between the organic PMMA core and the inorganic silica sensitive element, resulting in an unstable device with physical discontinuity between the optical fiber and the sensitive element.⁹

In this study we report the fabrication and characterization of a pH sensor based on an organic–inorganic hybrid matrix obtained by sol–gel process, doped with a pH sensitive dye, to be applied at the tip of plastic optical fibers. Inside the sensitive element, the organic part of the hybrid glass plays a multiple role: (i) it allows good adhesion between the plastic optical fiber and the whole sensitive element; (ii) it permits to tune the kinetic of response of the sensor by influencing the diffusion rate of the analyte inside the porous matrix and its interaction with the indicator; (iii) its nature of organic compound allows better physical and chemical interactions with the organic pH indicator dispersed in the hybrid matrix, thus reducing problems of leaching and enhancing the response rate of the sensor. The developed probe has been interrogated in reflectance mode. Optical effects, such as absorption and scattering, contribute to convert the pH of the solution into the spectral information. Thus, the pH value of the solution is obtained from the analysis of the spectrum of the back-scattered light.

In Sec. II, the working principle of the sensor is described. Section III deals with the realization of the probe; in Sec. IV the instrumentation and experimental activity are described and, finally, the main results are reported and discussed in Sec. V.

II. WORKING PRINCIPLE

The operating principle of the disposable sensor is based on the classical colorimetric approach. Consider the simple probe configuration reported in Fig. 1(a). The pH-sensitive dye is immobilized on the tip of the fiber and its color, related to the pH value of the solution, can be detected using a spectrometric approach. Indicators are weak acids or bases wherein the pH sensitivity is based on a color change. Thus, the information of interest is strictly associated with the selective absorption operated by the dye. A change in the color of the dye induces a change in the optical spectrum of the outgoing light collected by the fiber.

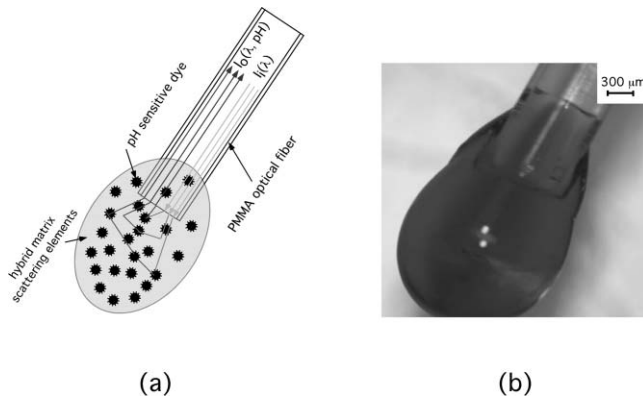


FIG. 1. Drawing of the probe configuration (a): $I_i(\lambda)$ is the interrogation light absorbed and scattered by the sensing hybrid matrix; $I_o(\lambda, pH)$ is the outgoing light containing the information of interest. (b) Picture of the sensing probes realized.

As the pH varies, the relative fractions concentrations of the dissociated $[A^-]$ and protonated $[HA^+]$ forms of the indicator are changed according to the Henderson–Hasselbalch equation:

$$pH = pK_a + \text{Log} \left(\frac{[A^-]}{[HA^+]}\right), \quad (1)$$

$$C = [A^-] + [HA^+],$$

where K_a is the acid dissociation constant, pK_a is $-\log K_a$, and C is the concentration of the indicator. According to Eq. (1), the concentrations of the relative fractions concentrations of the two forms can be easily calculated as a function of the pH value as

$$[HA^+] = \frac{C}{1 + 10^{pH-pK_a}}, \quad (2)$$

$$[A^-] = \frac{C}{1 + 10^{pK_a-pH}}.$$

According to Fig. 1(a), interrogation light $I_i(\lambda)$ is absorbed and scattered by the sensing matrix generating the outgoing light $I_o(\lambda, pH)$. Thus, although the polymer is chosen to be transparent in the range of absorption of the indicator dye, it should scatter light significantly. The spectrum of the outgoing light $I_o(\lambda, pH)$ can be estimated from the spectrum of the entering light $I_i(\lambda)$ using the modified Beer–Lambert law:¹⁰

$$OD(\lambda, pH) = \text{Log} \frac{I_i(\lambda)}{I_o(\lambda, pH)} = \alpha_A(\lambda) \cdot d(\lambda, pH) \cdot [A^-] + \alpha_{HA}(\lambda) \cdot d(\lambda, pH) \cdot [HA^+] + G, \quad (3)$$

$$OD(\lambda, pH) = C \cdot d(\lambda, pH) \cdot \left\{ \frac{\alpha_A(\lambda)}{1 + 10^{pK_a-pH}} + \frac{\alpha_{HA}(\lambda)}{1 + 10^{pH-pK_a}} \right\} + G,$$

where $OD(\lambda, pH)$ is the optical density, $\alpha_A(\lambda)$ and $\alpha_{HA}(\lambda)$ the specific extinction coefficients of the two forms, $d(\lambda, pH)$ the mean optical path of the photons through the probe, and G a parameter related to the “geometry” of the probe.

Hence, we consider the relative variations of the outgoing light as the sensor response:

$$\Re(\lambda, pH) = \frac{I_o(\lambda, pH_{\text{ref}}) - I_o(\lambda, pH)}{I_o(\lambda, pH)} = \frac{\Delta I_o(\lambda, pH)}{I_o(\lambda, pH)},$$

$$= \frac{\Delta OD(\lambda, pH)}{\text{Log}(e)}, \quad (4)$$

$$\Re(\lambda, pH) = \frac{C \times d(\lambda, pH)}{\text{Log}(e)} \times \left\{ \frac{\alpha_A(\lambda)}{1 + 10^{pK_a-pH}} + \frac{\alpha_{HA}(\lambda)}{1 + 10^{pH-pK_a}} \right\} - Bl(\lambda, pH_{\text{ref}}),$$

where baseline Bl is

$$Bl(\lambda, pH) = \frac{C \times d(\lambda, pH_{\text{ref}})}{\text{Log}(e)} \times \left\{ \frac{\alpha_A(\lambda)}{1 + 10^{pK_a-pH_{\text{ref}}}} + \frac{\alpha_{HA}(\lambda)}{1 + 10^{pH_{\text{ref}}-pK_a}} \right\}, \quad (5)$$

and pH_{ref} is the reference value of pH that annulls response $\Re(\lambda, pH)$.

III. PREPARATION OF THE DISPOSABLE PROBES

The sensor is based on a low-cost plastic (PMMA) fiber (Fort Fibre Ottiche, Italy) with core diameter 1 mm and numerical aperture 0.22. The total length of the taken fiber is 35 cm. The sensing matrix takes advantage of the use of organic–inorganic hybrids obtained from sol–gel technique by the use of polymeric organic phases bearing terminal reactive groups for the hydrolysis–condensation reactions that transform the precursor of the inorganic glass (namely TEOS) into the metal–alkoxide network (namely the silica glass). In this work, PEOs (α, ω -triethoxysilane-terminated polyethylene oxides) were used as the polymer chains to be covalently included in the silica glass. The resulting materials, also known as ceramers, give a unique combination of the properties of inorganic glasses (chemical and thermal stability, transparency, low coefficient of thermal expansion, etc.) with those of the organic polymer (ductility, gas or liquid permeability, etc.) included in the formulation of the hybrid material.

Polyethylene oxide (PEO) was chosen as the organic phase of the hybrids, thanks to its thermodynamic affinity with PMMA (necessary to obtain good adhesion between the plastic optical fiber and the dye-doped sensitive element), and the organic–inorganic weight ratio was varied in order to evaluate the influence of this parameter on the rate of response of the sensor and the capacity of permanent entrapment of the pH indicator molecules. Different molecular weights of PEO were selected and tested (in the range between 1000 and 8000 g/mol), in order to evaluate a possible effect of the polymer chain length on the entrapment and stabilization of the pH indicator; in principle, longer polymer chains should give rise to larger organic domains within the sol–gel hybrid structure, thus having higher capability of embedding and more numerous interactions with the organic indicator molecules, that should limit or avoid its leaching from the hybrid formulation. Samples were coded as follows: $PEOx-a:b\text{-dye}$ where x represents the molecular weight of the PEO chains used as organic component in the hybrid, $a:b$ indicates the organic:inorganic

weight ratio in the hybrid, and *dye* indicates the *pH* indicator entrapped in the hybrid structure (PR: Phenol red). For instance, sample named PEO1000-8:2-PR is a phenol red-doped organic-inorganic hybrid having 80% by weight of organic PEO phase ($M_w = 1000$ g/mol) and 20% by weight of silica phase. PEOSi/SiO₂ hybrids were prepared by dissolving TEOS (Sigma Aldrich, Milan, Italy) and PEOSi (prepared by reacting hydroxy-terminated PEO in bulk at 120 °C with 3-isocyanatopropyltriethoxysilane, all reactants purchased from Sigma Aldrich, Milan, Italy) in EtOH at a concentration of about 60% (w/v), and then adding water and HCl to promote hydrolysis and condensation reactions. Then *pH* indicators were dissolved into the mixture (approx 4 mg/50 ml) and left under stirring at room temperature for 15 min. The homogeneous dye-doped mixture was finally heated at 60 °C for 15–30 min (in order to approach the gel point) before the application of a drop onto the tip of the optical fiber.

The disposable sensors were cast by depositing a drop of hybrid sol onto the tip of the optical fibers, then the fibers were dried at atmospheric pressure and room temperature for 2 h and then cured at 105 °C for 60 h. In respect of a thin film deposition of the sensing matrix,¹¹ drop sensing probe allows us to obtain a larger mean optical path of the photons and thus, according to Eq. (4), an enhanced sensor response.

Different combinations of *PEOx-a:b-dye* have been studied to determine the best behavior in terms of adhesion between the optical fiber and the hybrid sensitive element, faster swelling, response rate and stable entrapment of the dye molecules. Figure 1(b) shows a typical sensing probe realized.

IV. INSTRUMENTS AND MEASUREMENTS

The interrogation of the sensing probe has been performed using the instrumental setup depicted in Fig. 2. The beam generated by the white light source (WLS) (tungsten halogen lamp, HL-2000-HF, Avantes, Netherlands) is delivered to the fiber-optic collimator FC1 (PAF-SMA-5-550, OFR, USA) through a 0.5 m long multimode optical fiber (1 mm core diameter, NA 0,51, Fort Fibre Ottiche, Italy). The resulting collimated light feeds the cube beam splitter (BS) (039-1130, Optosigna, USA). Light transmitted through BS is refocused by the second fiber-optic collimator FC2 (PAF-SMA-5-550, OFR, USA) into the fiber sensor, having the sensitive tip submerged into the testing solution. The *pH* of this solution is monitored by a *pH* electrode (Jenway 3045 Ion Analyser, Dunmore, UK).

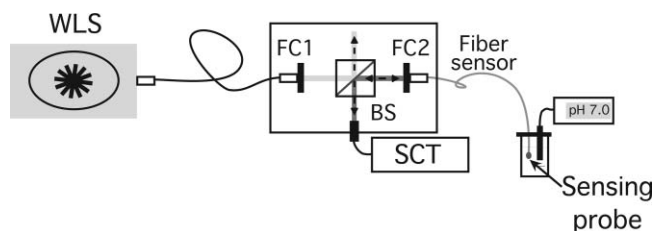


FIG. 2. Instrumental setup used for the interrogation of the sensing probe: WLS: tungsten halogen lamp, FC1 and FC2: fiber-optic collimators, BS: cube beam splitter, SCT: grating spectrometer. A *pH* electrode meter monitors the *pH* of the test solution.

The outgoing coloured light from the fiber sensor retraces the entering beam to BS that deflects part of it to the entrance fiber bundle of the grating spectrometer SCT (PMA-11 C5966, Hamamatsu, Japan) equipped with a charge-coupled device detector. The measuring spectral range covers the visible spectrum from 400 to 800 nm. Spectral resolution can be defined according to the Rayleigh criterion that indicates how wide the spectral distance between two lines must be to allow their recognition as separate lines. Here, the spectral width of the individual lines must be markedly smaller than their spacing. In our spectrometer, the maximum resolution achievable is easily computable dividing the spectral range by the number of acquisition spectral channels, i.e., 400 nm/820 = 0.487 nm. This theoretical limit does not take into account channels cross talk and other nonidealities.

All measurements were carried out at room temperature and the probes were not conditioned before use.

The first experiment was devoted to determine the spectral response of the interrogation system. Even though we measure signal variations, the spectral properties of the outgoing light should not be too corrupted by the response of the measuring system and transmission of the sensing POF. The experimental setup used for this characterization is shown in Fig. 3. First, the light spectrum $\tilde{I}_i(\lambda)$ at the output of a 35 cm-long POF without sensing matrix was measured using spectrometer SCT [Fig. 3(a)]. Afterward, the spectrometer was reassembled as in Fig. 3(b) using the same 35 cm-long POF. In front of the POF a National Institute of Standards and Technology calibrated reflectance target ($\mathfrak{S} = 99\%$, Labsphere, USA) acted as a lambertian diffuser. This target has a spectrally flat ($\pm 4\%$) reflectance over the UV-near-infrared spectrum. Spectrum $I_o(\lambda)$ acquired by SCT can be calculated as

$$I_o(\lambda) = k \times \mathfrak{S} \times S_r(\lambda) \times \tilde{I}_i(\lambda), \quad (6)$$

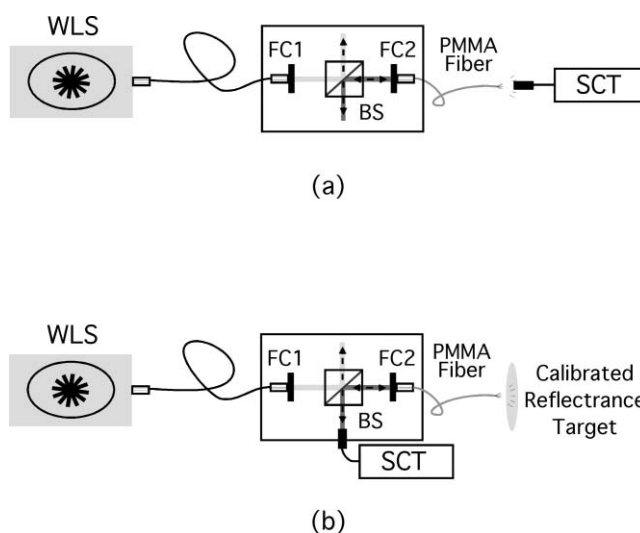


FIG. 3. Experimental setup used to measure the spectral response of the interrogation system. (a) The light spectrum at the output of a 35 cm-long POF without sensing matrix was measured. (b) Afterward, the spectrometer was reassembled and in front of the POF a calibrated reflectance target acted as a diffuser.

where is a coupling constant, \mathfrak{R} the calibrated target reflectance assumed not dependent on the wavelength, and $S_r(\lambda)$ the interrogation system response. Therefore, the ratio $I_o(\lambda)/\tilde{I}_i(\lambda)$ has been used to study the spectral trend of the interrogation system response.

Response $\mathfrak{R}(\lambda, pH)$ of the disposable sensors was evaluated by immersing the sensitive tip of the POF in 20 ml of a sample solution. Measurement was taken 5 min after changing the pH level that was controlled using standard pH buffers from 4–10 (Fisher Scientific). The testing solution was also continuously monitored with the reference pH meter, which has a measuring uncertainty of 0.05 units. A reference spectrum $I_o(\lambda, pH_{ref})$ was acquired at $pH_{ref} = 10$ and the values of the system response $\mathfrak{R}(\lambda, pH)$ were calculated varying the pH from 9 to 4.

Temporal response of the probe to a rapid change in pH has been investigated first visually inspecting the color changes and then acquiring continuously the spectrum $I_o(\lambda, pH_{ref})$ and calculating $\mathfrak{R}(\lambda, pH)$ as a function of time. The pH value of the solution has been staircase decreased from 8 to 5 with unitary steps of duration 10 s each. The same protocol has been applied to the reverse direction of the staircase, i.e., from 5 to 8. During these measurements too, the testing solution was continuously monitored with the reference pH meter.

V. RESULTS AND DISCUSSION

The sensing mechanism used in this disposable sensor relies on the photon diffusion process in the hybrid drop and on the absorption of the indicator. Both these processes are pH dependent and modify the spectrum of the outgoing light $I_o(\lambda, pH_{ref})$ and, thus, the response of the sensor $\mathfrak{R}(\lambda, pH)$. Notice how the size of the hybrid drop depends on the pH level of the solution and thus, varying the pH of the solution, the photon diffusion process produces different photon optical paths. By way of example, Fig. 4 shows the two shapes appearance of the probe PEO8000–8:2-PR after 5 min of im-

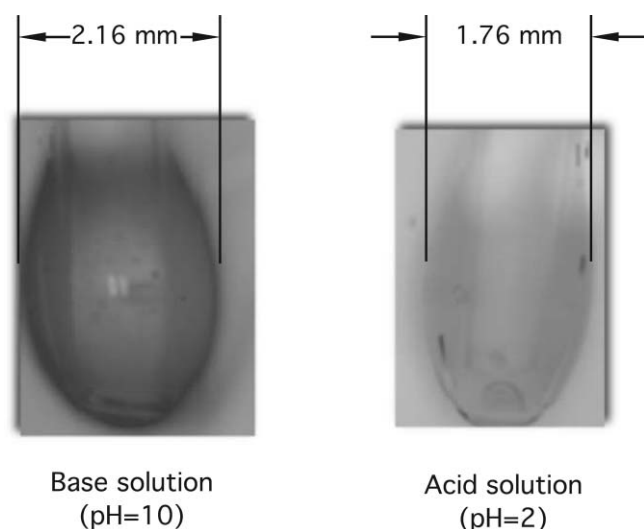


FIG. 4. Two shapes appearance of the probe PEO8000–8:2-PR after 5 min of immersion in basic (a) and acid (b) solutions.

mersion in a basic ($pH = 10$) and an acid ($pH = 2$) solution. Although reversibility is not strictly necessary for a disposable sensor, this hybrid probe provides advantages in terms of reversibility even though the response and recovery times are strictly related to the swelling/shrinking process that is pH dependent.

Phenol red has a limited solubility in the hybrid gel matrix; therefore, the leaching of the dye from the probe may occur. Varying x , a , and b in the matrix composition, this leaching process can be controlled. The best behavior, also in terms of adhesion to the optical fiber and response rate, was found using the PEO with the highest molecular weight (namely 8000 g/mol) in hybrids containing 80 wt. % of organic phase, i.e., PEO8000–8:2-PR. Actually, for this sensing matrix, no leaching of the dye was observed; however, the high molecular weight PEO significantly increased the recovery times of the gel. The swelling in water and the deswelling in air of the hybrid matrix take almost 3 and 10 min, respectively, to reach the half of the maximum.

A. Spectral response of the interrogation system

Spectra $I_o(\lambda)$, $\tilde{I}_i(\lambda)$ and their ratio are shown in Fig. 5. In Fig. 5(a) the upper dashed line represents the emission spectrum of the halogen lamp WLS. The comparison between this spectrum and $\tilde{I}_i(\lambda)$ well denotes the transmission features of the POF that showed an attenuation peak at about 750 nm.¹² Other distortions of the halogen lamp spectrum are related to the transmission properties of the optical components used in the interrogation setup.

Figure 5(b) shows the ratio $I_o(\lambda)/\tilde{I}_i(\lambda)$ that, according to Eq. (6), is proportional to the spectral response of the interrogation system. The spectral region of interest in our application is 500–600 nm, i.e., green–yellow–red; here, as shown in Fig. 5(b), the response of the interrogation system is satisfactorily flat, thus the information of interest is not corrupted.

B. Spectral properties of the probe

The response of the disposable sensor depends on proton activity and, thus, on the pH level. The spectra $\Delta I_o(\lambda, pH) = I_o(\lambda, pH) - I_o(\lambda, pH_{ref})$ acquired at different value of pH are shown in Fig. 6. The light absorption of phenol red is clearly evident at the wavelength of 560 nm. According to the literature,¹³ at this wavelength the phenol red molecules exhibit a very low absorption that can be enhanced by increasing the pH of the solution. Hence, the specific extinction coefficient of the protonated form $\alpha_{HA}(560 \text{ nm})$ can be neglected with respect to that of the dissociated form $\alpha_A(560 \text{ nm})$ and Eq. (4) calculated at $\lambda = 560 \text{ nm}$ and $pH_{ref} = 10$ becomes

$$\mathfrak{R}(560 \text{ nm}, pH) = \frac{C \times d(560 \text{ nm}, pH)}{\text{Log}(e)} \times \left\{ \frac{\alpha_A(560 \text{ nm})}{1 + 10^{pK_a - pH}} \right\} - Bl(560 \text{ nm}, pH_{ref}). \quad (7)$$

From Fig. 6, it is clear that the swelling/shrinking process induces a change in the amplitude of the whole spectrum. This effect is described in Eq. (3) by parameter $d(\lambda, pH)$.

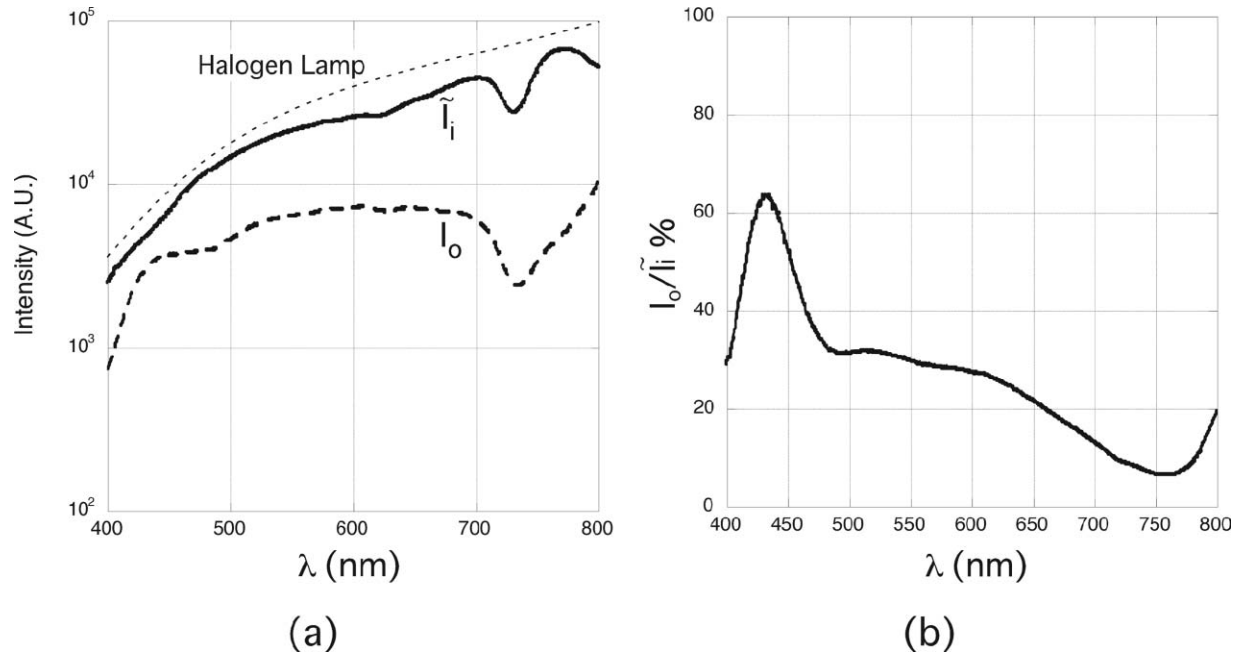


FIG. 5. Spectra of $\tilde{I}_i(\lambda)$ and $I_o(\lambda)$ (a), and spectral response of the interrogation system (b). In (a), the upper dashed line represents the emission spectrum of the halogen lamp WLS. The spectral region of interest for our application is 500–600 nm.

Let us consider typical spectrum $\Delta I_o(\lambda)$ shown in Fig. 7. To quantify the response of the sensor, we considered the characteristic parameters A and S calculated as follow: (i) the two maxima $M_1 = (\lambda_1, I_1)$, $M_2 = (\lambda_2, I_2)$ and the minimum $m = (\lambda_3, I_3)$ of $\Delta I_o(\lambda)$ have been calculated using a standard MATLAB routine; (ii) the equation of the line joining M_1 and M_2 has been calculated as $L(\lambda) = [(I_2 - I_1)/(\lambda_2 - \lambda_1)](\lambda - \lambda_1)$; (iii) A has been defined as $L(\lambda_3) - I_3$ and S as $L(\lambda_3)$. As shown in Fig. 7, parameter A is strictly related

to the absorption (at about $\lambda = 560$ nm) performed by the indicator, whereas S is correlated to the spectrum amplitude and, thus, to the swelling/shrinking process. For each spectrum acquired, parameters A and S were calculated; the normalized results plotted against pH are shown in Figs. 8(a) and 8(b). A shows a sharp transition as the pH of the solution changed from 5 to 8. The experimental data was fitted by the Boltzmann (sigmoidal) function according to Eq. (7). The point of inflection (sigmoidal fitting function equal to 0.5)

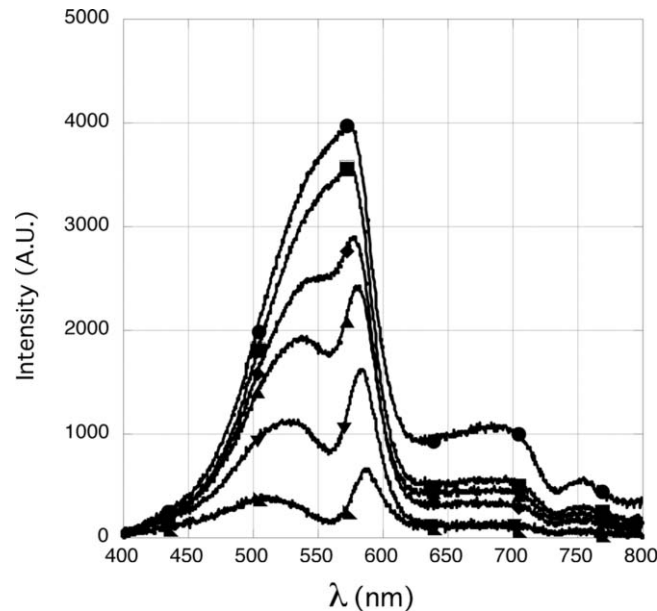


FIG. 6. Spectra of $\Delta I_o(\lambda)$ acquired at different values of pH: (●) pH 4, (■) pH 6, (▲) pH 7, (▼) pH 8, and (x) pH 9. The light absorption of phenol red is well visible at the wavelength of 560 nm. Swelling/shrinking process induces a change in the amplitude of the whole spectrum.

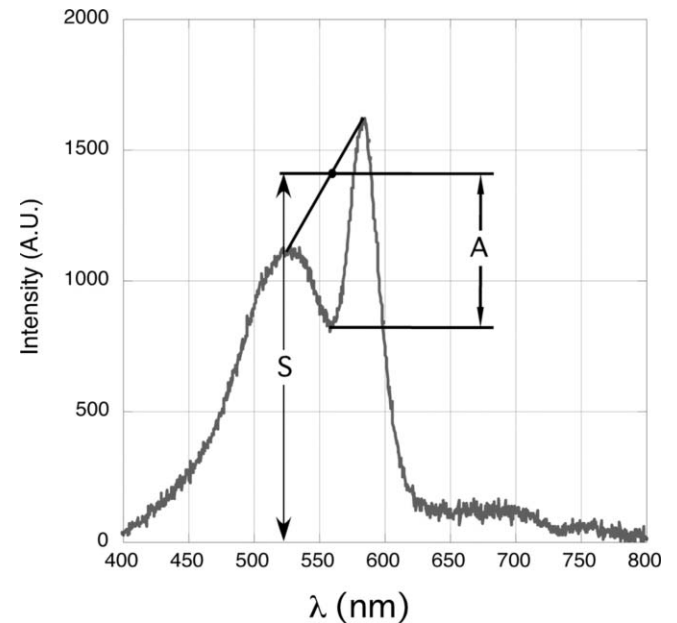


FIG. 7. Graphical definition of the two characteristic parameters. Parameter A is strictly related to the absorption performed by the indicator, whereas S is correlated to the swelling/shrinking process.

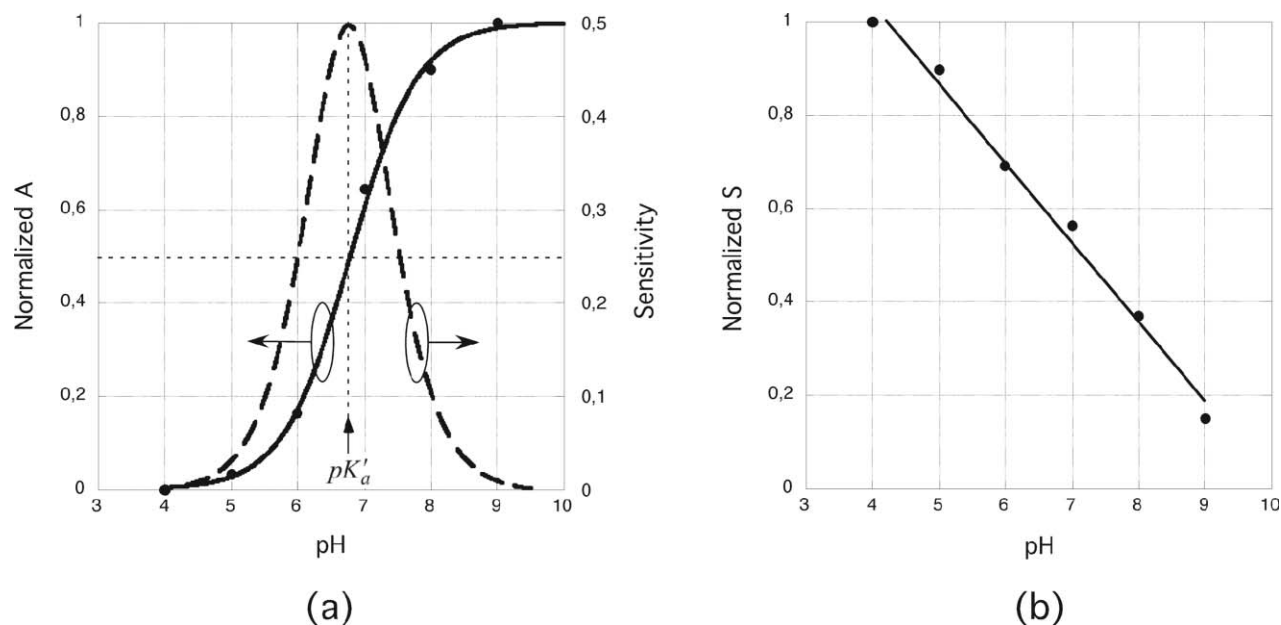


FIG. 8. Normalized A and S as a function of the pH value. Absorption parameter A is fitted by the Boltzmann function (a). The maximum sensitivity of the probe is 0.5. Linear fit of the normalized S exhibits a slope of 0.17 (b).

corresponds to the apparent pK_a values $pK'_a = 6.8$. This value is lower than the respective $pK_a = 7.9$ of phenol red in aqueous solution.¹⁴ As observed by Holobar *et al.*,¹⁵ the pK_a value can be shifted to lower pK with increasing ionic strength; this phenomenon could occur also in our hybrid matrix.

The sensitivity of the probe, calculated as the slope of the sigmoidal fitting function at the pK'_a value, is 0.5.

As shown in Fig. 4, visual inspection of the probe demonstrated a swelling process increasing the value of pH. We observed that this process tends to reduce the distance between the fiber tip and the probe-liquid interface. Therefore, mean optical path of the photons through the probe $d(\lambda, pH)$ decreased and, according to Eq. (4), also the sensor response diminished. Coherently, as shown in Fig. 8(b), parameter S decreased linearly with the pH of the solution. The linear fit of the experimental data exhibits a slope of 0.17.

C. Temporal response

The response time of the probe PEO8000-8:2-PR was measured. Optimization of the dye leaching and adhesion between the sensitive matrix and the POF require high molecular weight PEO that causes long response time of the sensor. Preliminary visual observations have demonstrated that when the pH was altered from 10 to 3, the color of the sensitive probe reached its steady state in a short time, i.e., less than 2 s. Alteration of pH from a low value to a high one resulted in longer response times that can be quantified in the order of some minutes, i.e., the kinetics depends on the direction of the pH change. This agrees with the results reported in literature.^{16,17} Quantification of these observations is shown in Fig. 9. In this figure, the parameter A (bold line), calculated as in Sec. IV, is represented as a function of time. In the same figure, the

value of the reference pH value (dashed line) of the solution is also shown. From a high to a low value of pH, the sensor was found to reach 90% of the regime signal intensity (τ_{90}) between 1 and 2 s. When the pH was changed from a low to a high value, the 90% of the regime signal intensity was not reached in the time scale of the experiment (10 s per step), except for the step between pH 5 and pH 6. In other words, we can observe two time constants describing: (i) a fast response with time scale similar to that observed for the high to low value of pH changes and (ii) a slow response. The regime signal intensity of each step for the staircase pH increasing was estimated from the mean signal values observed at the

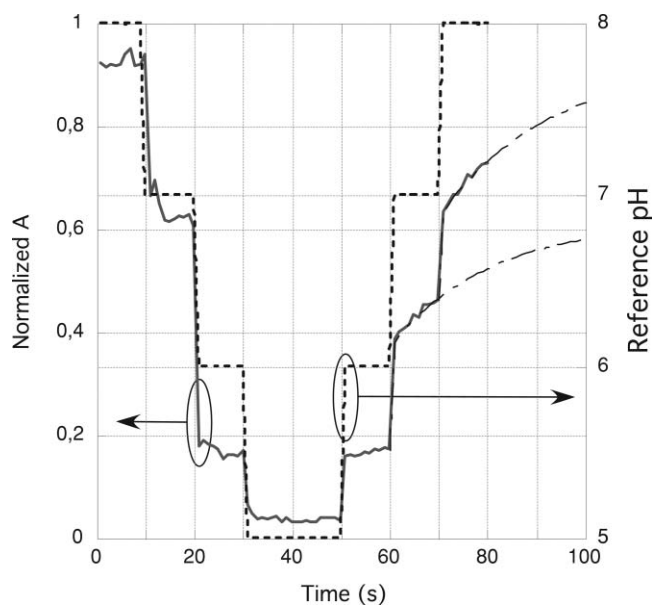


FIG. 9. Parameter A (—) and the value of the reference pH (dashed line) as a function of time. Each of the signal step variations 6 to 7 and 7 to 8 have been fitted with a double exponential function (dot-dashed line).

TABLE I. Figures of merit of the developed disposable pH sensor.

Parameter	Value
Measuring parameter	Absorbance at 560 nm
Probe diameter	2 mm typ.
Measuring pH range	5–8
Sensitivity	0.5 a.u./pH unit max
Response time	pH 8 to pH 5: 2 s max pH 5 to pH 8: 4 min typ.
Reusability	1 month
Mean lifetime	2 days
Cost	less than 0.7 Euro

same pH value during the staircase pH decreasing. Thus each signal step variation, i.e., 6 to 7 and 7 to 8, has been fitted with a double exponential function. The results of the fitting are shown in Fig. 9. Both the variations exhibited a fast response constant time of 0.28 s and a slow one in the order of 21–22 s.

When an alteration of pH from a low value to a high one occurs, the response time is dominated by the slow response of the probe. We assume that the slow response time observed when the pH was altered from 5 to 8 is strictly related to the swelling/shrinking kinetics of the sensitive drop. This experiment shows that the size of the sensitive drop depends not only on the pH but also on the swelling/shrinking kinetics that can be altered by the direction of the pH change.

The developed disposable sensor based on a low-cost plastic fiber exhibits a sigmoidal shape response function that covers an important pH range for physiological applications, e.g., in medicine and biotechnology, with excellent sensitivity. The reusability, tested with a series of probes checked once a day at a pH level in the middle of the range and preserved dry, has a mean life of 1 month. The mean lifetime of disposable

sensors, checked in the continuous mode operation at the pH level in the middle of the range, is 2 days. Table I shows these and other analytical parameters.

Some other advantages of the proposed sensor are: small size, high resistance to aggressive environments, and electrical isolation.

- ¹R. M. Durham, and J. A. Weigelt, *Surg. Gynecol. Obstet.* **169**(1), 14 (1989).
- ²O. A. Young, R. D. Thomson, V. G. Merhtens, and M. P. F. Loeffen, *Meat Sci.* **67**, 107 (2004).
- ³A. S. Jeevarajan, S. Vani, T. D. Tazlor, and M. M. Anderson, *Biotechnol. Bioeng.* **78**, 467 (2002).
- ⁴C. Schroeder, B. M. Weidgans, and I. Klimant, *Analyst* (Cambridge, U.K.) **130**, 907 (2005).
- ⁵A. Dybko, W. Wroblewski, E. Rozniecka, K. Poznaki, J. Maciejewski, R. Romaniuk, and Z. Brzozka, *Sens. Actuators B* **51**, 208 (1998).
- ⁶C. R. Blass, *Polymers in Disposable Medical Devices: A European Perspective* (Rapra Technology Ltd., U.K., 1999).
- ⁷B. D. MacGraith, V. Ruddy, C. Potter, B. O'Kelly, and J. F. McGilp, *Electron. Lett.* **27**, 1247 (1991).
- ⁸W. Cao and Y. Duan, *Sens. Actuators B* **110**, 252 (2005).
- ⁹J. Lin, *Trends Anal. Chem.* **19** (9), 541 (2000).
- ¹⁰R. Splinter and B. A. Hooper, *An Introduction to Biomedical Optics* (Taylor & Francis, London, 2006).
- ¹¹D. Galbarra, F. J. Arregui, I. R. Matias, and R. O. Claus, *Smart Mater. Struct.* **14** (4), 739 (2005).
- ¹²<http://www.fort.it/Catalogo%20FORT%20F.O.-CAVI%20& ACCESSORI.pdf>.
- ¹³E. Wang, K. F. Chowa, V. Kwan, T. Chin, C. Wong, and A. Bocarsly, *Anal. Chim. Acta* **495**, 45 (2003).
- ¹⁴S. Budavari, M. J. O'Neil, A. Smith, and P. E. Heckelman, *The Merck Index*, 11th ed. (Merck & Co., Inc. Rahway, NJ, 1989), p. 1551.
- ¹⁵A. Holobar, B. H. Weigl, W. Trettnak, R. Benes, H. Lehmann, N. V. Rodriguez, A. Wollschlager, P. O'Leary, P. Raspor, and O. S. Wolfbeis, *Sens. Actuators B* **11**, 425 (1993).
- ¹⁶F. Ismail, C. Malins, and N. J. Goddard, *Analyst* (Cambridge, U.K.) **127**, 253 (2002).
- ¹⁷G. E. Badini, K. T. V. Grattan, and A. C. C. Tseung, *Analyst* (Cambridge, U.K.) **120**, 1025 (1995).